JACS Au
AN OPEN ACCESS JOURNAL OF THE AMERICAN CHEMICAL SOCIETY

pubs.acs.org/jacsau
Article

Signaling Mechanism of Cuproptosis Activating cGAS-STING Immune Pathway

Chengyuan Zhu, Jialiang Li, Wanying Sun, Desheng Li, Yiliang Wang, and Xing-Can Shen*

Cite This: JACS Au 2024, 4, 3988−3999
Read Online

ACCESS | Metrics & More | Article Recommendations | Supporting Information

ABSTRACT: Copper-mediated programmed cell death, which influences the regulation of tumor progression, is an effective approach for antitumor molecular therapy. Unlike apoptosis, copper complex-induced cuproptosis by lipid-acylated protein aggregation triggers the mitochondrial proteotoxic stress response, which could be associated with immunomodulation. However, it remains a great challenge to understand the distinctive molecular mechanisms that presumably activate immunity by cuproptosis. Here, the new nonlabeling fluorescent molecular tools of Cu-DPPZ-Py$^+$ and Cu-DPPZ-Ph are synthesized and used to investigate the differential immune signaling mechanisms induced by copper-mediated cuproptosis or apoptosis. With Cu-DPPZ-Py$^+$ and Cu-Elesclomol, there is strong evidence that the triggering cuproptosis significantly drives mitochondrial DNA (mtDNA) release to activate innate immunity via cyclic GMP-AMP synthase-stimulation of interferon genes (cGAS-STING), which can improve T cell antitumor immunity *in vivo*. By contrast, it is observed that Cu-DPPZ-Ph treated tumor cells could release intracellular caspase-3, resulting in apoptosis-associated immunosuppression. This study supports insights into how cuproptosis bridges cGAS-STING immune pathways, contributing to the development of cuproptosis-based antitumor immunotherapy.

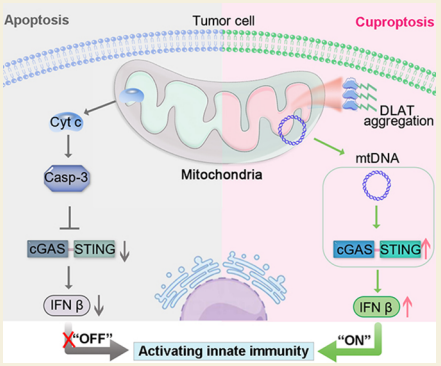

KEYWORDS: *Cuproptosis, apoptosis, cGAS-STING, innate immunity, molecular tools*

INTRODUCTION

Programmed cell death plays a crucial role in regulating tumor progression, and is an effective approach to antitumor molecular therapy.[1,2] Traditional platinum-based drugs, such as cisplatin (CDDP), are of great importance in antitumor therapy by inducing apoptosis via binding to DNA, and interfering with the cell's DNA replication and repair processes.[3,4] Although highly effective, platinum-based drugs are limited by dose-dependent systemic toxicities and chemoresistance.[3,4] Copper complexes have been investigated based on the assumption that copper as an essential metal may be less toxic with respect to antitumor.[5,6] In previous studies, copper complexes-mediated apoptosis primarily through DNA cross-linking followed by inhibition of DNA transcription and replication.[5−8] Although apoptosis is the main pathway of cell death induced by copper-based antitumor reagents, the low antitumor immune responses still restrict the clinical prospect of cancer immunotherapy.[9,10]

As a nonapoptotic pathway, cuproptosis has been identified as a copper-dependent cell death.[11] Cuproptosis is characterized by excess copper directly binding to lipoylated components of the tricarboxylic acid cycle, inducing aggregating lipoylated proteins and losing the Fe−S cluster, resulting in mitochondrial proteotoxic stress.[11−17] Notably, mitochondria are central regulators of immune homeostasis and may act as a potent immunomodulator,[18−20] so it has been considered that cuproptosis is related to immune response.[21−24] Recently, the copper-based nanosystem has been found to stimulate the intracellular cyclic GMP-AMP synthase-stimulator of interferon genes (cGAS-STING) pathway.[25−27] However, the current explorations of cuproptosis-mediated immune pathway signaling are mostly nanosystems. The mechanistic study of molecular agents is fundamental to the development of novel antitumor drugs. Cu-Elesclomol is widely recognized as a molecular tool to induce cuproptosis.[11,12] However, the lack of fluorescent properties poses obstacles to exploring organelle-associated immune homeostasis.[18,19] Moreover, the development of more copper ionophores can deepen the understanding of copper-induced cell death-related immune mechanisms, which is critical for optimizing copper-based drug design and expanding the application outlook.[12] Therefore, it is a great challenge to investigate the distinctive mechanisms that presumably activate immunity by cuproptosis using appropriate molecular tools.

Received: August 7, 2024
Revised: September 12, 2024
Accepted: September 12, 2024
Published: September 20, 2024

Scheme 1. Molecular Tools Structure of Cu-DPPZ-Py$^+$ and Cu-DPPZ-Ph and Schematic Illustration of How Cuproptosis Drives Mitochondrial DNA (mtDNA) Release to Activate Immunity via Cyclic GMP-AMP Synthase Stimulation of Interferon Genes (cGAS-STING)[a]

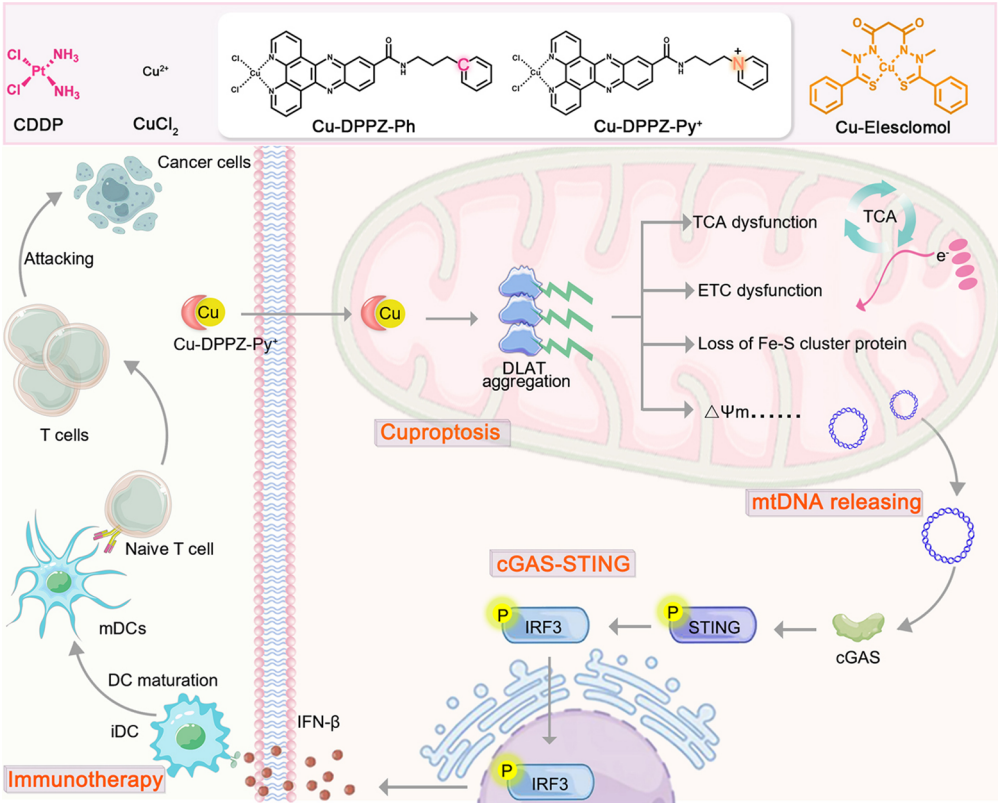

[a]Cisplatin (CDDP), apoptosis inducer; Cu-Elesclomol, cuproposis inducer.

In this work, the conventional apoptosis inducer (dipyridophenazine copper complex, Cu-DPPZ),[28,29] acting as a coordination core, is modified with phenyl group (Ph) and pyridine cation group (Py$^+$) to obtain two structurally similar copper complexes (Cu-DPPZ-Ph and Cu-DPPZ-Py$^+$). Interestingly, the intrinsic fluorescence signal shows that Py$^+$ imparts mitochondria-targeting properties to Cu-DPPZ-Py$^+$ compared to Cu-DPPZ-Ph, which contributes to mitochondrial Cu overloading and thus effectively triggers cuproptosis. Thus, Cu-DPPZ-Ph and Cu-DPPZ-Py$^+$ can be used as new molecular tools to explore the different signaling mechanisms of cuproptosis or apoptosis on immune pathways. It has been discovered that cuproptosis-induced lipoylated protein aggregation leads to mitochondrial dysfunction and the release of mitochondrial DNA (mtDNA) to the cytoplasm (Scheme 1). In contrast to apoptosis-associated immunosuppression, cuproptosis activates innate immunity via the cGAS-STING pathway. Subsequently, the secretion of type I interferon (IFN) and expression of IFN-β are upregulated, which promotes dendritic cell (DC) maturation and evokes robust innate immunity. Moreover, cuproptosis-associated innate immunity activates T-cell immunity, contributing to antitumor immunotherapy. Herein, this study demonstrates that cuproptosis can induce innate immune responses via the cGAS-STING pathway with new molecular tools, providing an efficient approach for developing cuproptosis-based molecular agents for cancer immunotherapy.

RESULTS AND DISCUSSION

Synthesis of Copper Complexes as Molecular Tools to Induce Cuproptosis or Apoptosis

In previous reports, Cu-DPPZ (DPPZ: dipyrido[3,2-a:2′,3′-c]phenazine) induces apoptosis through its DNA binding and cleavage properties.[28,29] With Cu-DPPZ as the coordination core, two copper complexes were synthesized based on carbon-to-nitrogen single-atom transmutation of the molecular skeleton, ensuring their structural similarity. The DPPZ-Ph ligand (N-(3-phenylpropyl)dipyrido[3,2-a:2′,3′-c]phenazine-11-carboxamide) was composed of a DPPZ (dipyrido[3,2-a:2′,3′-c]phenazine), an amide linker, and a phenyl group (−Ph). Similarly, the DPPZ-Py$^+$ ligand (1-(3-(dipyrido[3,2-a:2′,3′-c]phenazine-11-carboxamido)propyl)pyridin-1-ium) was composed of DPPZ (dipyrido[3,2-a:2′,3′-c]phenazine), an amide linker, and a pyridine cation group (−Py$^+$). Cu-DPPZ-Ph and Cu-DPPZ-Py$^+$ were synthesized and characterized by ^{1}H NMR, 2D ^{1}H−^{1}H COSY, and Mass spectra (Figures S1 and S2). As shown in Figure S3, DPPZ-Ph and DPPZ-Py$^+$ ligands did not present obvious toxicity within a certain range, consistent with previous reports.[30−32] Whereas, Cu-DPPZ-Ph and Cu-DPPZ-Py$^+$ were able to effectively inhibit the tumor cells after coordination. In addition, Cu-DPPZ-Ph and Cu-DPPZ-Py$^+$ possessed fluorescent properties without additional modification (Figure S4A and S4B) and hold the potential to carry out mitochondrial localization analysis via cellular fluorescence imaging. Then, colocalization analysis with mitochondrial probes and the intrinsic fluorescence of the

https://doi.org/10.1021/jacsau.4c00712
JACS Au 2024, 4, 3988−3999

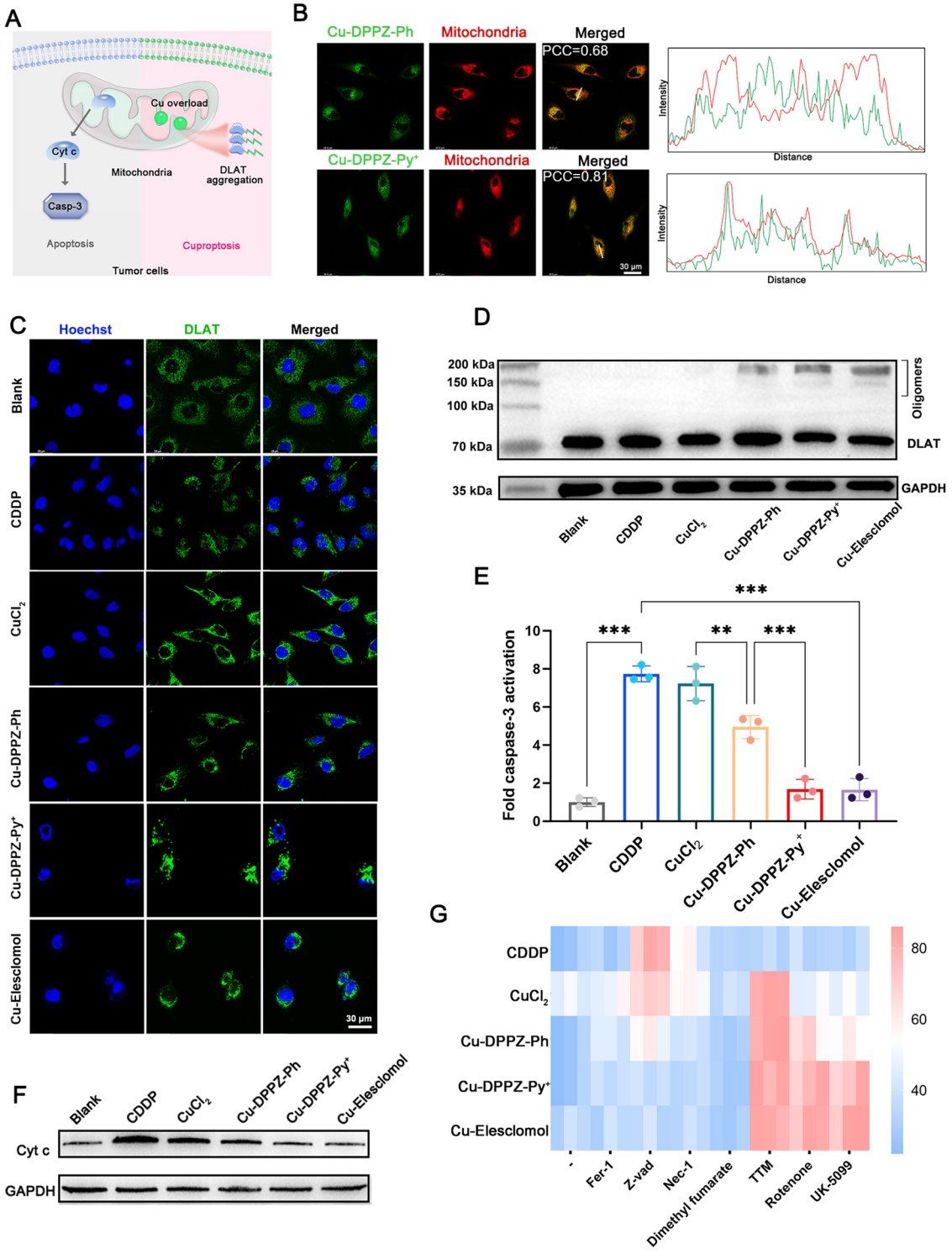

Figure 1. (A) Cuproptosis is characterized by dihydrolipoamide *S*-acetyltransferase (DLAT) aggregation. In the apoptotic pathway, Cyt c release triggers the activation of caspase-3. (B) Analysis of colocalization of copper complexes with mitochondria in HeLa cells. Green, Cu-DPPZ-Ph or Cu-DPPZ-Py$^+$; red, mitochondria. Scale bar: 30 μm. PCC: Pearson correlation coefficient. (C) Immunofluorescence staining imaging of DLAT oligomerization in HeLa cells after different treatments. Green, DLAT; blue, nucleus. Scale bar: 30 μm. (D) Western blot analysis of DLAT oligomerization in 4T1 cells. (E) Caspase-3 activity was measured in 4T1 cells after different treatments. (F) Cyt c levels in the cytoplasm were detected by Western blotting. (G) Viability of 4T1 cells pretreated with inhibitors of different death modes followed by different treatments for 24 h.

copper complexes revealed that Cu-DPPZ-Py$^+$ possessed a better Pearson's colocalization factor compared to Cu-DPPZ-Ph (Figure 1B). Cu-DPPZ-Py$^+$ was able to effectively achieve copper accumulation in mitochondria compared to Cu-DPPZ-Ph (Figure S4C). Thus, carbon-to-nitrogen single-atom transmutation of the molecular skeleton with Cu-DPPZ as the coordination core led to structural similarity and charge differences of copper complexes. Meanwhile, Cu-DPPZ-Py$^+$

https://doi.org/10.1021/jacsau.4c00712
JACS Au 2024, 4, 3988−3999

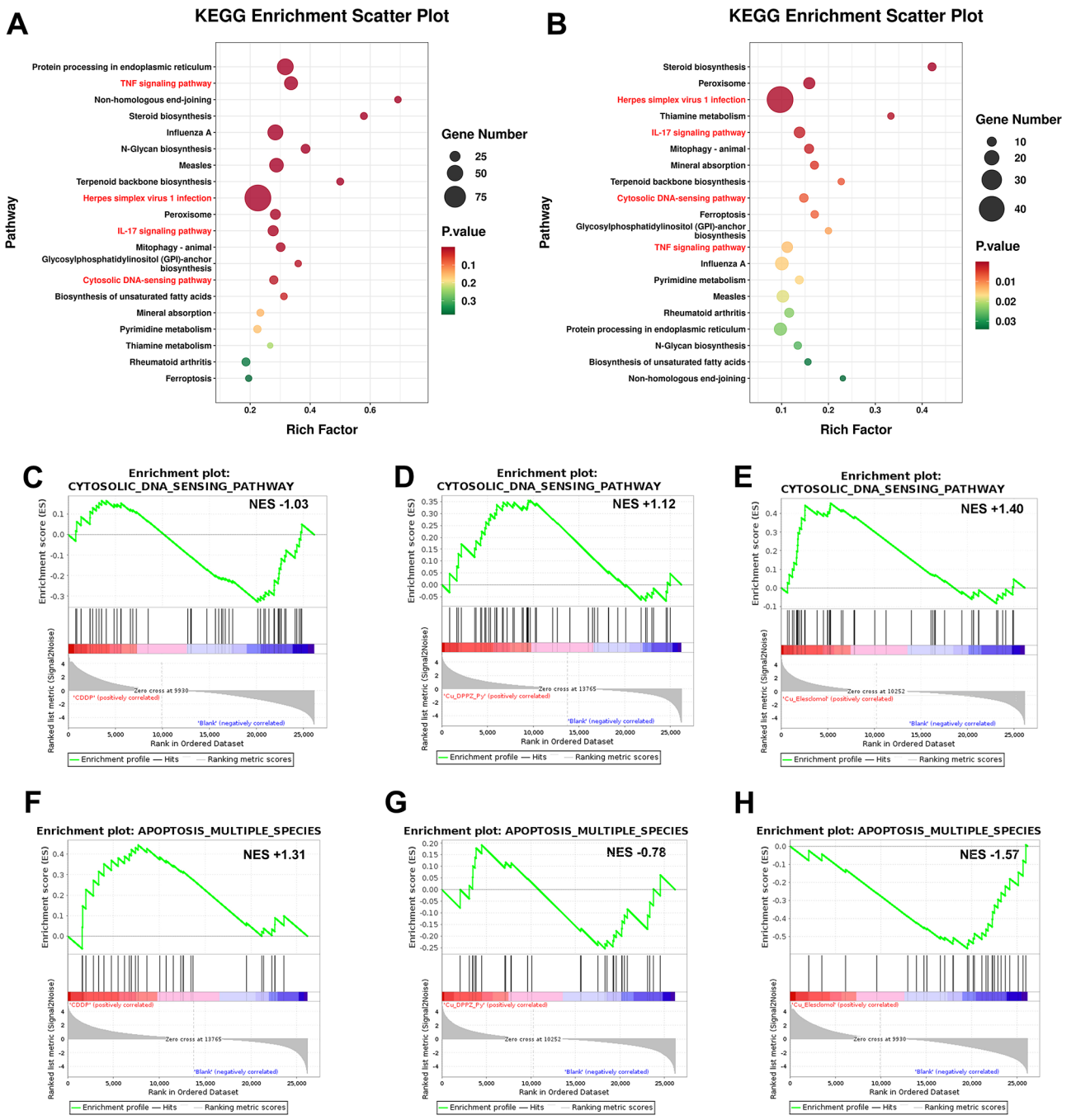

Figure 2. RNA-seq analysis of 4T1 cells treated with CDDP, Cu-DPPZ-Py$^+$, and Cu-Elesclomol. KEGG analysis of differentially expressed genes between cells treated with (A) Cu-DPPZ-Py$^+$ and (B) Cu-Elesclomol. GSEA analysis (Cytoplasmic DNA-sensitive pathway) of differentially expressed genes in cells subjected to (C) CDDP, (D) Cu-DPPZ-Py$^+$, and (E) Cu-Elesclomol. GSEA analysis (apoptosis-multiple species) of differentially expressed genes in cells subjected to (F) CDDP, (G) Cu-DPPZ-Py$^+$, and (H) Cu-Elesclomol.

effectively targeted mitochondria compared to Cu-DPPZ-Ph based on the intrinsic fluorescent signal.

The formation of DLAT oligomers is an important feature of cuproptosis.[33−35] Western blot analysis was performed to investigate the DLAT proteins in the tumor cells. Besides a clear DLAT signal at 70 kDa, DLAT aggregation signals were also present at around 200 kDa after Cu-DPPZ-Py$^+$ and Cu-DPPZ-Ph treatment consistent with cuproptosis inducer Cu-Elesclomol (Figure 1D). Furthermore, Cu-DPPZ-Py$^+$ showed significant DLAT aggregation compared to free copper ions and Cu-DPPZ-Ph, demonstrating the importance of mitochondria in the process of cuproptosis. Meanwhile, immunofluorescence staining showed a uniform distribution of fluorescent signals in the cytoplasm of untreated cells, while significant aggregation of fluorescent signals appeared in cells treated with Cu-DPPZ-Py$^+$ (Figure 1C). These data demonstrated that Cu-DPPZ-Py$^+$ with mitochondrial targeting could indeed induce significant DLAT aggregation for cuproptosis, compared to Cu-DPPZ-Ph (Figure 1A).

Leakage of cytochrome c (Cyt c) from mitochondria into the cytoplasm activates caspase-3, which is the classical molecular event of apoptosis.[10] To investigate the ability of Cu-DPPZ-Py$^+$ and Cu-DPPZ-Ph to induce apoptosis, the cytoplasmic Cyt c levels were assessed via Western blot

https://doi.org/10.1021/jacsau.4c00712
JACS Au 2024, 4, 3988−3999

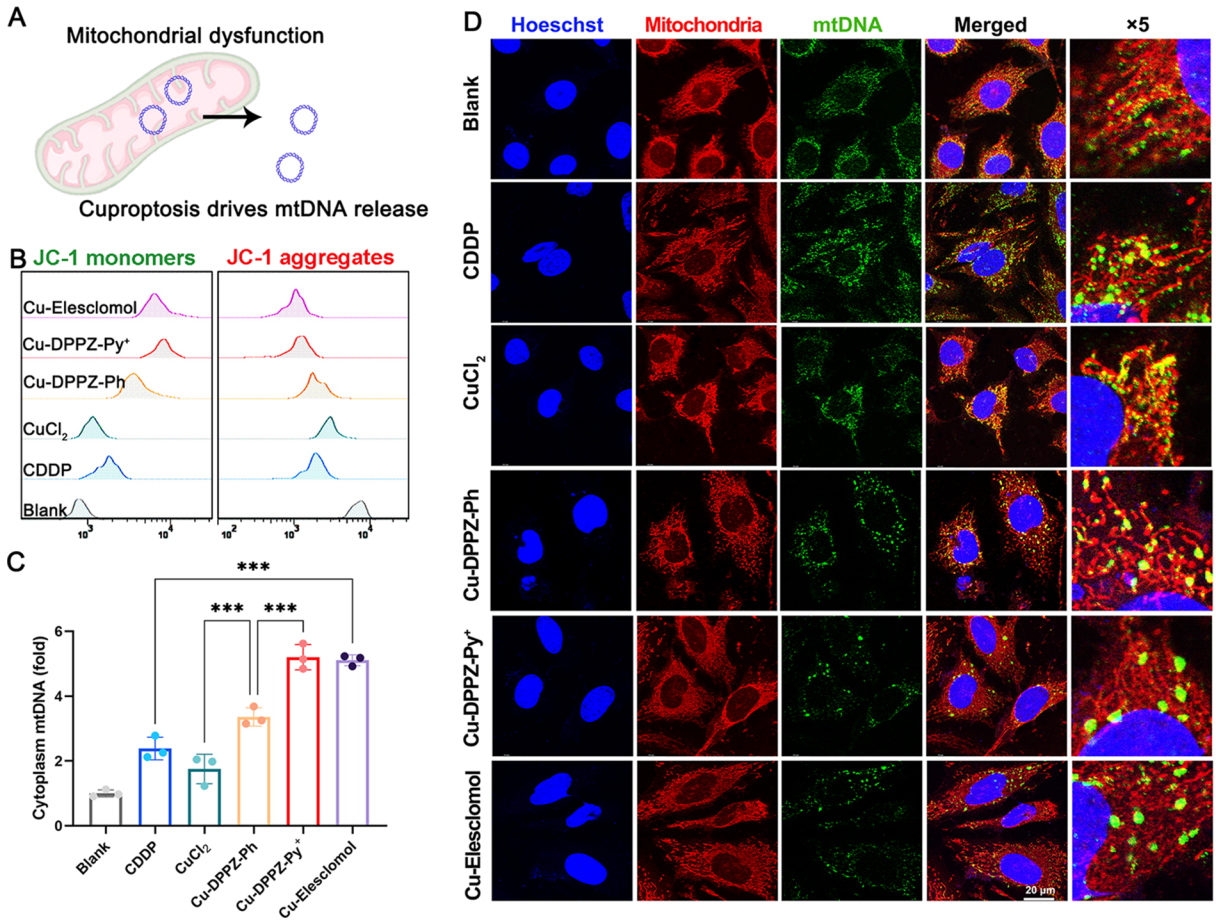

Figure 3. Evaluation of mtDNA release during cuproptosis or apoptosis. (A) Cuproptosis drove mtDNA release from mitochondria into the cytoplasm. (B) Mitochondrial membrane potential was analyzed by flow cytometry in 4T1 cells under different treatments. (C) mtDNA was extracted from the cytoplasm of 4T1 cells and analyzed by RT-qPCR. (D) Immunofluorescence staining imaging of mtDNA release in HeLa cells. Blue: nucleus. Scale bar: 20 μm.

analysis. As shown in Figure 1E, Cu-DPPZ-Ph did evoke an up-regulation of cytoplasmic Cyt c levels consistent with traditional apoptosis inducers (CDDP), whereas Cu-DPPZ-Py$^+$ showed no significant alteration. Then, an assessment of caspase-3 activity was performed by analyzing fluorescence changes in Ac-DEVD-AMC.[36] Ac-DEVD-AMC is a tetrapeptide compound that specifically binds to and cleaves caspase-3, resulting in the release of free AMC (7-aminomethylcoumarin) to generate a fluorescent signal. Figure 1F shows that cells treated with Cu-DPPZ-Ph establish significant fluorescence intensity consistent with CDDP, indicating activation of caspases-3. These data showed that Cu-DPPZ-Ph was inclined to activate apoptosis pathways compared to Cu-DPPZ-Py$^+$.

To further explore the mechanism of copper complex-induced cell death, cell death inhibitors (Z-vad, Nec-1, Fer-1, dimethyl fumarate) were used specifically to block apoptosis, necroptosis, ferroptosis, and pyroptosis, respectively.[11,37] As shown in Figure 1G, these inhibitors did not prevent Cu-DPPZ-Py$^+$-induced cell death, whereas Z-vad (apoptosis blocking) was able to alleviate Cu-DPPZ-Ph-induced cell death. Importantly, Cu-DPPZ-Py$^+$-induced cell death was reversible with three cuproptosis inhibitors: TTM (copper ion chelator), UK 5099 (inhibitor of mitochondrial pyruvate uptake), and Rotenone (inhibitor of electron transport chain), in line with Cu-Elesclomol.[11,38] Meanwhile, Cu-DPPZ-Ph-mediated cell death was mitigated to some extent by the cuproptosis inhibitors. This suggested that Cu-DPPZ-Ph induced apoptosis and cuproptosis, whereas Cu-DPPZ-Py$^+$ acted as a cuproptosis inducer without activating the apoptotic pathway. It was shown that carbon-to-nitrogen single-atom transmutation of the molecular skeleton increased the positive electrical properties of the copper complexes, which was the key to the tendency of inducing mitochondria-dependent cuproptosis by Cu-DPPZ-Py$^+$. Therefore, Cu-DPPZ-Ph and Cu-DPPZ-Py$^+$ could be used as structurally similar and fluorescent molecular tools to explore the presumably immune-related molecular mechanisms of copper-mediated cuproptosis or apoptosis.

RNA-Seq Analysis of Tumor Cells during Cuproptosis or Apoptosis

To comprehensively investigate whether cuproptosis or apoptosis was capable of activating immune signaling and the corresponding mechanisms, RNA-seq analysis was performed. Considering the excellence of the cuproptosis or apoptosis inducer, RNA-seq analysis was performed on 4T1 cells treated with Cu-Elesclomol, Cu-DPPZ-Py$^+$, and CDDP.

Differential genes induced by cuproptosis inducer (Cu-DPPZ-Py$^+$ and Cu-Elesclomol, 693 Cu-DEGs) were screened as per the Venn diagram (Figure S5D). Differentially expressed genes were further analyzed via the Kyoto Encyclopedia of Genes and Genomes (KEGG) analysis to explore their

https://doi.org/10.1021/jacsau.4c00712
JACS Au 2024, 4, 3988−3999

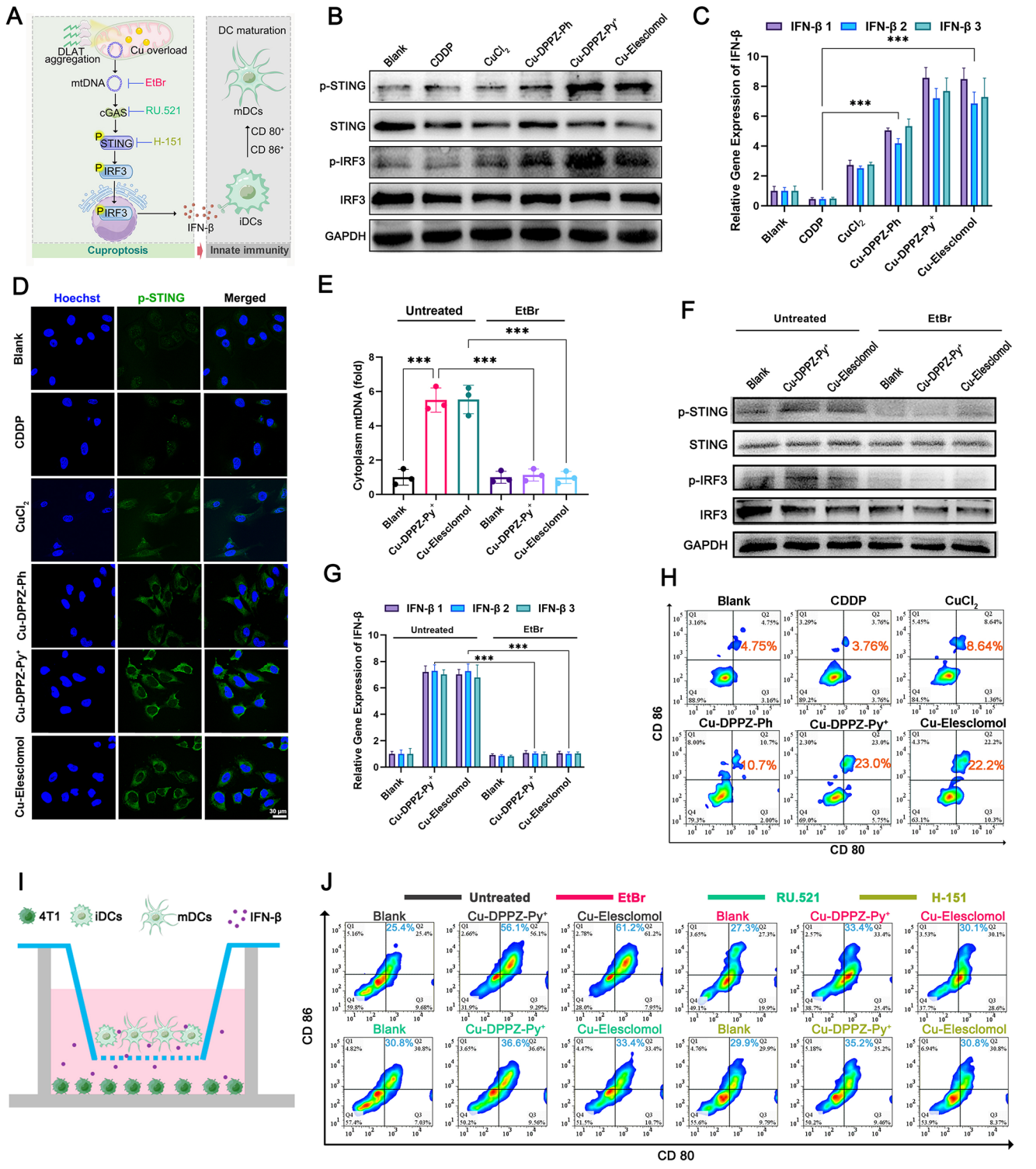

Figure 4. (A) Potential mechanism of cuproptosis activating innate immunity. Immature dendritic cells, iDCs; mature dendritic cells, mDCs. (B) Protein expression of cGAS-STING in 4T1 cells. (C) mRNA expression of the cytokines IFN-β in 4T1 cells under different treatments was analyzed by RT-qPCR using three different primers. (D) Confocal images of p-STING levels in HeLa cells with different treatments. Scale bar: 30 μm. (E) The relative amount of mtDNA in the cytoplasm was assessed by RT-qPCR. (F) cGAS-STING-related protein expression and (G) mRNA expression of the cytokines IFN-β in 4T1 and 4T1 ρ^0 cells under different treatments. (H) Flow cytometry analysis of BMDCs maturation induced by culture medium supernatant of tumor cells. (I) The transwell system was utilized to explore the maturation of DCs induced by different treatments for tumor cells. The upper layer is DCs and the lower layer is 4T1 cells. (J) The maturation of BMDCs was induced by culture medium supernatant of tumor cells pretreated with inhibitors.

function. Compared to apoptosis inducer (CDDP), screening of the top TOP20 pathways enriched in cuproptosis inducer showed significant enrichment in the TNF signaling pathway, Herpes simplex virus 1 infection, IL-17 signaling pathway, and Cytosolic DNA-sensing pathway (Figure 2A,B and Figure S5E). Subsequently, Cu-DEGs were analyzed via Gene

https://doi.org/10.1021/jacsau.4c00712
JACS Au 2024, 4, 3988−3999

ontology (GO). Biological processes (BP) showed that these Cu-DEGs were enriched in protein phosphorylation in addition to DNA-related stimulation, cell cycle, and positive and negative regulation of apoptosis. The cell component (CC) showed that these Cu-DEGs were enriched not only in the mitochondria, where cuproptosis occurred, but also in the nucleus and cytoplasm. In terms of molecular function (MF), these Cu-DEGs are enriched in protein binding, metal ion binding, ATP binding, etc., which was related to the protective mechanism of cells against cuproptosis (Figure S5F).

More importantly, gene set enrichment analysis (GSEA) showed that the cytosolic DNA sensing pathway was upregulated in cuproptosis compared to apoptosis (Figure 2C−E). Meanwhile, GSEA analysis showed that the cuproptosis-inducer-treated group did not activate the apoptotic pathway (Figure 2F−H). These data suggest that cuproptosis possessed the potential to activate inflammatory signaling through DNA-related pathways compared to apoptosis.

Evaluation of mtDNA Release from Mitochondria into the Cytoplasm during Cuproptosis or Apoptosis

mtDNA was once thought to be "foreign" and probably of bacterial origin, suggesting that it was considered different from the cell's "own" nucleus DNA and could act as powerful damage-associated molecular patterns (DAMPs).[39] Since cuproptosis-mediated proteotoxic stress disrupts mitochondrial integrity, mtDNA may be released from mitochondria into the cytoplasm. To explore this hypothesis, mitochondrial membrane potential was probed by the JC-1 assay. As shown in Figure 3B, cells treated with cuproptosis inducer (Cu-DPPZ-Py^+) showed stronger green and weaker red fluorescence compared to Cu-DPPZ-Ph, indicating the loss of mitochondrial membrane potential. Meanwhile, it showed that Cu-DPPZ-Py^+ induced mitochondrial membrane potential loss which could be mitigated by cuproptosis inhibitors (Figure S6). This suggests that cuproptosis was an important contributor to the Cu-DPPZ-Py^+-induced mitochondrial dysfunction.

Due to the lack of histone protection, mtDNA is easily released from mitochondria to the cytoplasm during mitochondrial stress.[20] Subsequently, mtDNA was detected by assessing the expression of the mtDNA-binding protein TFAM (Transcription Factor A, Mitochondrial).[40] Western blot analysis was employed to detect changes in TFAM protein expression levels. As shown in Figure S7, down-regulated TFAM was present in the Cu-DPPZ-Py^+ and Cu-Elesclomol. As shown in Figure 3D, the red fluorescently labeled mitochondria formed an elaborate network with a uniform distribution of green fluorescently labeled individual mtDNA in the steady state. Interestingly, the green-labeled mtDNA coalesced into discrete globular structures and was released into the cytoplasm, after treatment with cuproptosis inducer. To quantify the release of mtDNA, mtDNA was extracted from the cytoplasm and analyzed by real-time quantitative polymerase chain reaction (RT-qPCR). It showed that apoptosis indeed induced the release of mtDNA consistent with previous reports. The level of cytoplasmic mtDNA in cells treated with cuproptosis inducer Cu-DPPZ-Py^+ was significantly higher than that observed in cells treated with Cu-DPPZ-Ph (Figure 3C). Figure S8A illustrates that the relative content of cytoplasmic mtDNA gradually increased with the escalating concentration of Cu-DPPZ-Py^+. Furthermore, the cuproptosis inhibitor (TTM, UK 5099) significantly alleviated the release of mtDNA, suggesting that Cu-DPPZ-Py^+-induced mtDNA release was associated with cuproptosis (Figure S8B). Figure S8C shows that pharmacological inactivation of mitochondrial permeability transition pores (mPTP) using cyclosporin A (CSA) prevented Cu-DPPZ-Py^+ inducing mtDNA leakage into the cytoplasm. It indicated mtDNA release may be mediated through the mPTP.[41] These data suggest that cuproptosis facilitates mitochondrial dysfunction to release mtDNA from mitochondria into the cytoplasm compared with apoptosis.

Cuproptosis Drives Distinctive mtDNA-Mediated cGAS-STING Pathway for DC Maturation

The cGAS-STING pathway, a critical element of the innate immune system, senses cytoplasmic DNA and triggers a cascade of signaling that contributes to host defense against pathogens and the regulation of inflammatory responses.[42,43] Due to the cuproptosis inducing the enrichment of mtDNA in the cytoplasm, it created favorable conditions for activation of the cGAS-STING pathway.

To verify the activation of the cuproptosis-related cGAS-STING pathway, key events such as protein phosphorylation, including STING and IRF3 were analyzed by Western blot.[44−46] As shown in Figure 4B, Cu-DPPZ-Py^+ boosted the expression of p-IRF3 and p-STING proteins, consistent with Cu-Elesclomol. Cyclic GMP-AMP (cGAMP), also known as 2′3′-cyclic GMP-AMP, is a product of cyclic GMP-AMP synthase (cGAS) sensing cytoplasmic DNA and activates downstream immune responses by binding to stimulator of interferon genes (STING). As shown in Figure S9a, the content of cGAMP increased significantly after treatment with the cuproptosis inducers Cu-DPPZ-Py^+ and Cu-Elesclomol. To visualize the activation of intracellular cGAS-STING, immunofluorescence staining for p-STING (green) in HeLa cells was conducted. It observed that cells treated with cuproptosis inducer (Cu-DPPZ-Py^+ and Cu-Elesclomol) showed higher green fluorescence intensity than the Cu-DPPZ-Ph, which may be related to the inhibition of cGAS-STING by caspase-3 in the apoptosis pathway (Figure 4D). These results suggest that cuproptosis contributed to the cGAS-STING activation in contrast to apoptosis. Subsequently, medium supernatants from cells were used for IFN-β expression via an enzyme-linked immunosorbent assay (ELISA) kit. Notably, IFN-β was significantly increased in 4T1 tumor cells treated with the cuproptosis inducer via ELISA analysis (Figure S10. Exhilaratingly, mRNA expression of the cytokines IFN-β in the Cu-DPPZ-Py^+ groups was higher than that in Cu-DPPZ-Ph (Figure 4C). This observation suggested that distinct from apoptosis, cuproptosis-induced cytoplasmic mtDNA accumulation triggers the cGAS-STING, resulting in interferon secretion.

To investigate whether cuproptosis-activated cGAS-STING signaling was dependent on mtDNA release, a 4T1 cell line deficient in mtDNA (referred to as 4T1 ρ^0) was engineered. Ethidium bromide (EtBr) is a cationic lipophilic DNA-intercalating agent that binds specifically to mtDNA, potentially reducing mtDNA copy number during cell division.[41] After 3 weeks of incubation of 4T1 cells with EtBr, mtDNA release was assessed by RT-qPCR. As shown in Figure 4E, the cuproptosis inducer promoted the accumulation of mtDNA in the cytoplasm, while EtBr treatment significantly reduced the release behavior of mtDNA. This indicated that the 4T1 ρ^0 cell model was successfully constructed.

https://doi.org/10.1021/jacsau.4c00712
JACS Au 2024, 4, 3988−3999

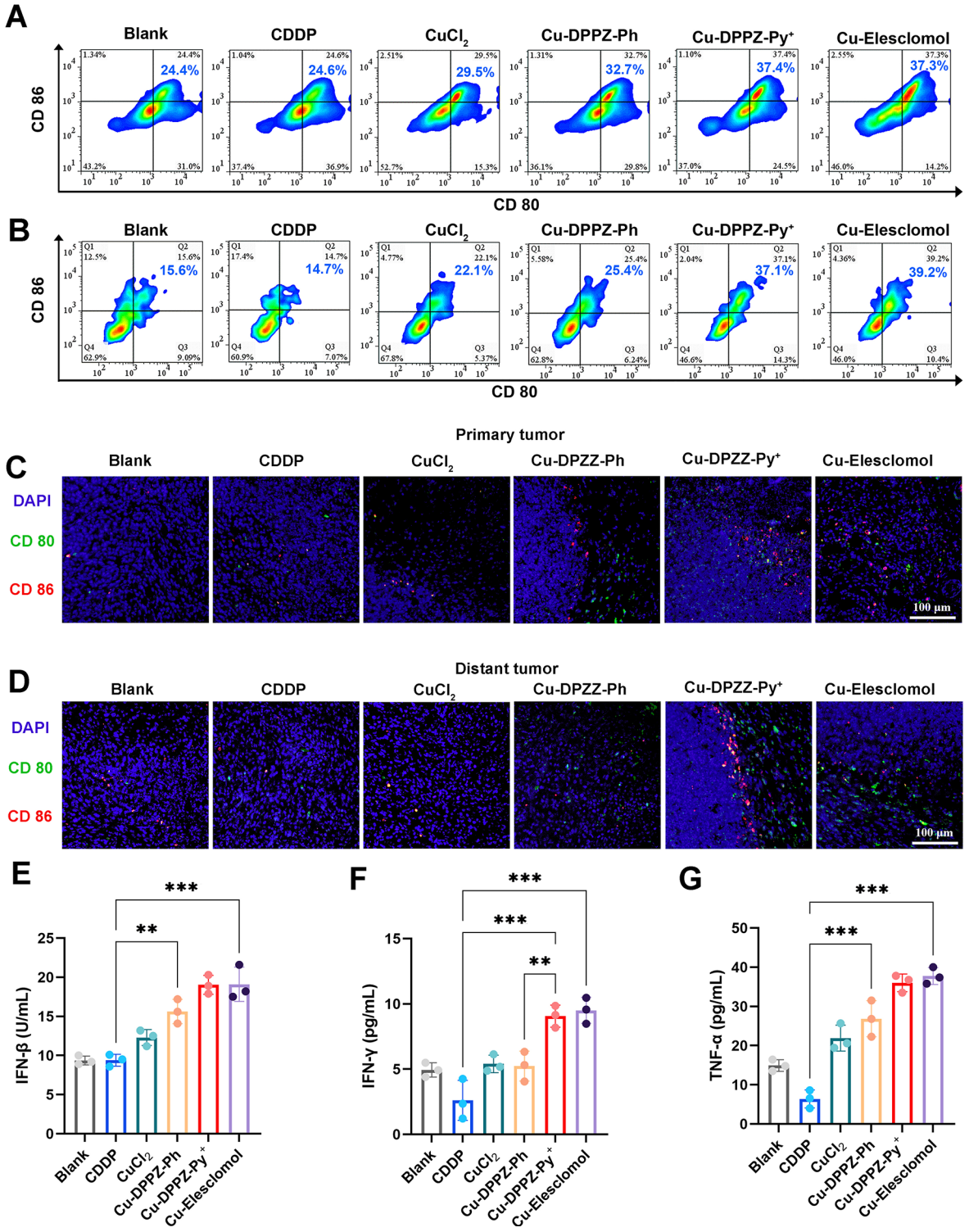

Figure 5. Flow cytometry analysis of DCs maturation at the (A) primary tumor site and (B) lymph node. Immunofluorescence images of (C) primary and (D) distant tumor sections for mature DCs stained with CD 86 (red), CD 80 (green), and nuclear (blue). Scale bars: 100 μm. Cytokine levels of (E) IFN-β, (F) IFN-γ, and (G) TNF-α in the serum of differently treated tumor-bearing mice.

Subsequently, the expression of signature proteins of the cGAS-STING pathway in 4T1 ρ^0 cells was assessed by RT-qPCR and a Western blot assay. As shown in Figure 4F, mtDNA deletion did not change the level of STING and IRF3 but significantly reduced the level of cuprottosis-mediated expression of p-STING and p-IRF3. mRNA expression of the cytokines IFN-β was measured by RT-qPCR. As shown in Figure 4G, EtBr-induced mtDNA depletion contributes to the downregulation of the gene expression of IFN-β in 4T1 ρ^0 cells undergoing cuproptosis. At the same time, EtBr-induced mtDNA deletion also resulted in a decrease in the cGAMP concentration (Figure S9b). These results evidenced that the cuproptosis-activated cGAS-STING pathway was closely linked to mtDNA release.

https://doi.org/10.1021/jacsau.4c00712
JACS Au 2024, 4, 3988−3999

Cuproptosis-activated cGAS-STING may contribute to subsequent immune responses. Differently treated 4T1 cells were cocultured with mouse bone marrow-derived dendritic cells (BMDCs) through the transwell system. BMDC maturation (CD 80+ CD 86+) was assessed by using flow cytometry. The cuproptosis inducer group showed significant upregulation of CD 80 and CD 86 compared to other treatments (Figure 4H). To further investigate whether cuproptosis inducted BMDCs maturation was dependent on cGAS-STING induced by mtDNA release in Ptumor cells, EtBr was used to deplete the mtDNA, H-151 was used to inhibit STING, and RU.521 was used to inhibit cGAS.[41] BMDCs maturation experiments showed that supernatants from EtBr and cGAS-STING inhibitor pretreated 4T1 cells undergoing cuproptosis did not cause upregulation of CD 80+ CD 86+ (Figure 4J). It showed that cuproptosis to activate BMDCs maturation was dependent on the mtDNA-cGAS-STING pathway. Therefore, different from the immuno silencing of apoptosis, cuproptosis could induce mtDNA release to activate the cGAS-STING pathway for DC maturation, indicating the potential of cuproptosis to activate innate immunity *in vivo*.

Cuproptosis Activates Innate Immunity *In Vivo*

Activation of cGAS-STING by cuproptosis prompted us to explore its potential to induce innate immunity *in vivo*. First, a bilateral 4T1 tumor model (right: primary tumor; left: distant tumor) was established. The expression of Cyt c and caspase-3 in tumor tissues was further examined. As shown in Figure S11, compared to cisplatin (CDDP), cuproptosis inducers did not significantly activate the release of Cyt c to trigger caspase-3 activation. The activation of the cGAS-STING pathway in tumor tissues was also evaluated. As shown in Figure S12, both Cu-Elesclomol and Cu-DPPZ-Py$^+$ caused upregulation of p-STING and p-IRF3, indicating that the cGAS-STING pathway was activated. To further confirm the immunostimulatory effect of cuproptosis, flow cytometry was used to analyze the status of DCs in tumors and tumor-draining lymph nodes (Figure 5A and B). A single intratumorally treatment with a cuproptosis inducer significantly contributed to the maturation of DCs (CD 80+ CD 86+) in tumors and tumor-draining lymph nodes, compared to apoptosis inducers. More interestingly, maturation increases of DCs were observed in Cu-DPPZ-Py$^+$ groups compared to the Cu-DPPZ-Ph groups, suggesting that mitochondrial targeting conferred by carbon−nitrogen single-atom transmutation was important for the activation of innate immunity by cuproptosis. The same conclusion was verified by evaluating immunofluorescence section staining images of primary and distant tumors (Figure 5C, D). In addition, serum IFN-β was elevated after the treatment with the cuproptosis inducer (Figure 5E). These results suggest that compared to apoptosis, cuproptosis-enhanced immunogenicity of tumor cells can indeed induce DC maturation *in vivo*, which is essential for activating the innate immune system.

Encouraged by the activation of the innate immune system by cuproptosis, we further assessed the ability to trigger adaptive immune responses was further assessed. Cytotoxic T cells (CD 3+ CD 8+) and helper T cells (CD 3+ CD 4+) in primary tumors, distant tumors, and tumor-draining lymph nodes were further evaluated via flow cytometry. Consistent with DC maturation, mice treated with cuproptosis inducers exhibited the highest T cell activation and infiltration, suggesting that cuproptosis-activated innate immunity contributed to the activation of T cell immunity (Figures S13−S15). After verification that cuproptosis activates T-cell immunity, proinflammatory cytokines in serum including IFN-γ and TNF-α, were measured by ELISA. The up-regulation of serum proinflammatory factors of the cuproptosis inducer demonstrated the activation of adaptive immunity (Figure 5F, 5G). At the end of 14 days of treatment, primary and distant tumor growth was successfully inhibited by the cuproptosis inducer (Figures S16 and S17), and no significant weight change was observed in mice (Figure S18). The Cu-DPPZ-Py$^+$ and Cu-DPPZ-Ph complexes were administered to mice via a single intratumoral injection. The copper concentrations in major organs (heart, liver, spleen, lung, and kidney) and plasma were measured by using inductively coupled plasma mass spectrometry (ICP-MS). As illustrated in Figure S19a and b, copper accumulation in the liver peaked 6 h after injection, higher than in other major organs. This suggested that these metal complexes are primarily metabolized through the liver in mice. Figure S19c and d demonstrates the coordination structure of Cu-DPPZ-Py$^+$ and Cu-DPPZ-Ph in plasma. The pharmacokinetic parameters were provided in Figure S19e. Compared with Cu-DPPZ-Ph, Cu-DPPZ-Py$^+$ was more readily absorbed, likely due to its positive charge and solubility. As shown in Figure S20, H&E staining of the heart, liver, spleen, lung, and kidney revealed that similar to the control group, the morphology of major organ cells in mice treated with Cu-DPPZ-Py$^+$ and Cu-DPPZ-Ph remained intact, with no evident organ damage or abnormal inflammatory signals observed. These results suggest that cuproptosis-mediated innate immunity contributes to the activation of adaptive immunity and has great potential for tumor immunotherapy *in vivo*.

CONCLUSIONS

In conclusion, this work demonstrates distinctive molecular mechanisms of cuproptosis, activating innate immunity via cGAS-STING with new molecular tools. These new non-labeling fluorescent copper complexes (Cu-DPPZ-Py$^+$ and Cu-DPPZ-Ph) are designed and synthesized, which trigger cuproptosis or apoptosis, respectively. Importantly, it significantly shows the Cu-DPPZ-Py$^+$-mediated cuproptosis activity in the cGAS-STING pathway, distinct from apoptosis. Moreover, the cuproptosis-associated innate immunity could activate T cell immunity, resulting in systemic antitumor immunotherapy and inhibition of tumors. In contrast, Cu-DPPZ-Ph-mediated apoptosis triggered the release of Cyt c to activate caspase-3, resulting in immunosuppression. Therefore, these results facilitate the understanding of cuproptosis-activated innate immunity and offer a rational design for developing copper-based molecular agents for antitumor immunotherapy.

METHODS

Cell Culture

HeLa and 4T1 cells were cultured in MEM and RPMI-1640 medium, respectively, supplemented with 10% FBS and 1% penicillin-streptomycin at 37 °C in a 5% CO_2 humidified atmosphere. mtDNA depletion was performed in a correlation medium containing 500 ng/mL ethidium bromide (EtBr), 100 μg/mL sodium pyruvate, and 50 μg/mL uridine. 4T1 cells were cultured in this medium for 2 weeks to obtain depleted cells (ρ^0) The relative copy numbers of mtDNA were detected by RT-qPCR.

https://doi.org/10.1021/jacsau.4c00712
JACS Au 2024, 4, 3988−3999

In Vitro Cytotoxicity Assay

Cells received different treatments (CDDP, $CuCl_2$, Cu-DPPZ-Ph, Cu-DPPZ-Py^+, and Cu-Elesclomol) for 24 h after morphological unfolding. Discard the old medium and then add 100 μL of medium with the Cell Counting Kit-8 (CCK-8) to each well. After incubation for 0.5−1 h, the absorbance at 450 nm wavelength of each well was measured by enzyme marker. The relative cell viability (%) was calculated by $(A_{test}/A_{control}) \times 100$. To investigate the influence of cuproptosis inhibitors on the cytotoxicity of Cu-DPPZ-Ph, Cu-DPPZ-Py^+, and Elesclomol-Cu, 4T1 cells were pretreated with 100 nM UK 5099, 100 nM Rotenone, and 200 μM TTM for 6 h, respectively. For cell death mechanisms analysis, 4T1 cells were pretreated with pan-caspase inhibitors (Z-VAD-FMK, 30 μM), ferroptosis inhibitors (ferrostatin-1, 10 μM), necroptosis inhibitors (necrostatin-1, 20 μM), and pyroptosis inhibitors (dimethyl fumarate, 20 μM) for 6 h, respectively.

Immunofluorescence Imaging

The cells were seeded in a confocal dish (1.0×10^4 cells per dish). Different drugs were added at their respective IC20 values after the cells were attached to the dish. After 24 h, the culture medium was discarded, and precooled TBS buffer was slowly added to the cells. The cells were then covered with 1 mL of 4% neutral formaldehyde fixative (prepared in TBS buffer) and placed at 4 °C for 15 min to fix. The fixative was removed, and the cells were washed three times with precooled TBS buffer for 5 min each time. Subsequently, cell permeabilization was performed to allow the antibodies to reach the antigen sites. The permeabilization agent used was 0.3% Triton X-100 (prepared in TBS buffer), and the permeabilization time typically ranged from 5−15 min. After cell membrane permeabilization, cells were washed three times with TBS for 5 min each. After being blocked at 37 °C for 60 min, cells were incubated with primary antibody at 4 °C overnight. Cells were washed three times with TBS and incubated with fluorescently labeled secondary antibody for 60 min at room temperature. After three washes with TBS, the cell nuclei were labeled with Hoechst 33342 for 15 min. It is worth noting that the labeling of mitochondria using a fluorescent probe (MitoTracker Deep Red FM, Yeasen Biotechnology (Shanghai) Co., Ltd.) must be performed before cell fixation.

BMDCs Maturation

Bone marrow-derived dendritic cells (BMDCs) were extracted from the tibia and femurs in BALB/c mice. Cells were collected by flushing the bone marrow cavity with sterile surgical instruments and a culture medium. After erythrocyte lysis, the cell suspension was centrifuged and resuspended in a culture medium. The medium was supplemented with 25 ng/mL of GM-CSF (Med Chem Express, US) and 15 ng/mL of IL-4 (Med Chem Express, US). The medium was changed every 3 days and is ready for further experiments after 7 days of incubation.

The 4T1 cells were seeded in the lower layer of the transwell experiment. Different drugs were added at their respective IC values of 20 after the cells were attached to the dish. After 12 h of treatment with different drugs, the old medium was replaced with a new medium and BMDCs were inoculated in the upper layer. After 2 days of incubation, the maturation rate of BMDCs was analyzed. The BMDCs were ground into single-cell suspension, stained with APC antimouse CD 11c, PE antimouse CD 86, and FITC antimouse CD 80 (BioLegend, America), and then detected by flow cytometry (BD Calibur).

■ ASSOCIATED CONTENT

Supporting Information

The Supporting Information is available free of charge at https://pubs.acs.org/doi/10.1021/jacsau.4c00712.

Experimental details including materials, methods, synthetic procedures, characterization data (NMR, HRMS, etc.), RT-qPCR quantification, flow cytometry, H&E staining, and additional figures (PDF)

■ AUTHOR INFORMATION

Corresponding Author

Xing-Can Shen − *State Key Laboratory for Chemistry and Molecular Engineering of Medicinal Resources, Key Laboratory for Chemistry and Molecular Engineering of Medicinal Resources (Ministry of Education of China), Collaborative Innovation Center for Guangxi Ethnic Medicine, School of Chemistry and Pharmaceutical Sciences, Guangxi Normal University, Guilin 541004, China;* orcid.org/0000-0002-7116-6919; Email: xcshen@mailbox.gxnu.edu.cn

Authors

Chengyuan Zhu − *State Key Laboratory for Chemistry and Molecular Engineering of Medicinal Resources, Key Laboratory for Chemistry and Molecular Engineering of Medicinal Resources (Ministry of Education of China), Collaborative Innovation Center for Guangxi Ethnic Medicine, School of Chemistry and Pharmaceutical Sciences, Guangxi Normal University, Guilin 541004, China*

Jialiang Li − *State Key Laboratory for Chemistry and Molecular Engineering of Medicinal Resources, Key Laboratory for Chemistry and Molecular Engineering of Medicinal Resources (Ministry of Education of China), Collaborative Innovation Center for Guangxi Ethnic Medicine, School of Chemistry and Pharmaceutical Sciences, Guangxi Normal University, Guilin 541004, China*

Wanying Sun − *State Key Laboratory for Chemistry and Molecular Engineering of Medicinal Resources, Key Laboratory for Chemistry and Molecular Engineering of Medicinal Resources (Ministry of Education of China), Collaborative Innovation Center for Guangxi Ethnic Medicine, School of Chemistry and Pharmaceutical Sciences, Guangxi Normal University, Guilin 541004, China*

Desheng Li − *State Key Laboratory for Chemistry and Molecular Engineering of Medicinal Resources, Key Laboratory for Chemistry and Molecular Engineering of Medicinal Resources (Ministry of Education of China), Collaborative Innovation Center for Guangxi Ethnic Medicine, School of Chemistry and Pharmaceutical Sciences, Guangxi Normal University, Guilin 541004, China*

Yiliang Wang − *State Key Laboratory for Chemistry and Molecular Engineering of Medicinal Resources, Key Laboratory for Chemistry and Molecular Engineering of Medicinal Resources (Ministry of Education of China), Collaborative Innovation Center for Guangxi Ethnic Medicine, School of Chemistry and Pharmaceutical Sciences, Guangxi Normal University, Guilin 541004, China*

Complete contact information is available at: https://pubs.acs.org/10.1021/jacsau.4c00712

Author Contributions

C.Z., J.L., and X.-C.S. designed the study. C.Z., J.L., and W.S. performed the experiments. C.Z., J.L., and D.L. processed the experimental data and designed figures and tables in the manuscript. C.Z., J.L., and X.-C.S. wrote the manuscript. X.-C.S. and Y.W. gave practical suggestions on the experiments and manuscript. X.-C.S. supervised the study. All authors approved the final manuscript.

Notes

The authors declare no competing financial interest.

■ ACKNOWLEDGMENTS

This work was supported by the National Natural Science Foundation of China (22377018), the BAGUI Scholar Program of Guangxi, and the National College Students'Innovation and Entrepreneurship Training Program (202210602038).

■ REFERENCES

(1) Bedoui, S.; Herold, M. J.; Strasser, A. Emerging connectivity of programmed cell death pathways and its physiological implications. *Nat. Rev. Mol. Cell Biol.* **2020**, *21*, 678−695.
(2) Nagata, S.; Tanaka, M. Programmed cell death and the immune system. *Nat. Rev. Immunol.* **2017**, *17*, 333−340.
(3) Kelland, L. The resurgence of platinum-based cancer chemotherapy. *Nat. Rev. Cancer* **2007**, *7*, 573−584.
(4) Wang, D.; Lippard, S. J. Cellular processing of platinum anticancer drugs. *Nat. Rev. Drug Discovery* **2005**, *4*, 307−320.
(5) Tardito, S.; Marchiò, L. Copper compounds in anticancer strategies. *Curr. Med. Chem.* **2009**, *16* (11), 1325−1348.
(6) Santini, C.; Pellei, M.; Gandin, V.; Porchia, M.; Tisato, F.; Marzano, C. Advances in copper complexes as anticancer agents. *Chem. Rev.* **2014**, *114* (1), 815−862.
(7) Gupta, T.; Dhar, S.; Nethaji, M.; Chakravarty, A. R. Bis(dipyridophenazine)copper(II) complex as major groove directing synthetic hydrolase. *Dalton Trans.* **2004**, 1896−1900.
(8) Rochford, G.; Molphy, Z.; Kavanagh, K.; McCann, M.; Devereux, M.; Kellett, A.; Howe, O. Cu(II) phenanthroline-phenazine complexes dysregulate mitochondrial function and stimulate apoptosis. *Metallomics* **2020**, *12* (1), 65−78.
(9) Meier, P.; Legrand, A. J.; Adam, D.; Silke, J. Immunogenic cell death in cancer: targeting necroptosis to induce antitumour immunity. *Nat. Rev. Cancer.* **2024**, *24*, 299−315.
(10) Ning, X.; Wang, Y.; Jing, M.; Sha, M.; Lv, M.; Gao, P.; Zhang, R.; Huang, X.; Feng, J.−M.; Jiang, Z. Apoptotic caspases suppress type I interferon production via the cleavage of cGAS, MAVS, and IRF3. *Mol. Cell* **2019**, *74* (1), 19−31.
(11) Tsvetkov, P.; Coy, S.; Petrova, B.; Dreishpoon, M.; Verma, A.; Abdusamad, M.; Rossen, J.; Joesch-Cohen, L.; Humeidi, R.; Spangler, R. D.; Eaton, J. K.; Frenkel, E.; Kocak, M.; Corsello, S. M.; Lutsenko, S.; Kanarek, N.; Santagata, S.; Golub, T. R. Copper induces cell death by targeting lipoylated TCA cycle proteins. *Science* **2022**, *375* (6586), 1254−1261.
(12) Wang, W.; Mo, W.; Hang, Z.; Huang, Y.; Yi, H.; Sun, Z.; Lei, A. Cuproptosis: harnessing transition metal for cancer therapy. *ACS Nano* **2023**, *17* (20), 19581−19599.
(13) Xu, S.; Hao, Y.; Xu, X.; Huang, L.; Liang, Y.; Liao, J.; Yang, J.; Zhou, Y.; Huang, M.; Du, K.−Z.; Zhang, C.; Xu, P. Antitumor activity and mechanistic insights of a mitochondria-targeting Cu(I) complex. *J. Med. Chem.* **2024**, *67* (10), 7911−7920.
(14) Tang, D.; Kroemer, G.; Kang, R. Targeting cuproplasia and cuproptosis in cancer. *Nat. Rev. Clin. Oncol.* **2024**, *21*, 370−388.
(15) Yang, Y.; Li, M.; Chen, G.; Liu, S.; Guo, H.; Dong, X.; Wang, K.; Geng, H.; Jiang, J.; Li, X. Dissecting copper biology and cancer treatment: 'activating cuproptosis or suppressing cuproplasia'. *Coord. Chem. Rev.* **2023**, *495*, No. 215395.
(16) Li, Y.; Guo, Y.; Zhang, K.; Zhu, R.; Chen, X.; Zhang, Z.; Yang, W. Cell death pathway regulation by functional nanomedicines for robust antitumor immunity. *Adv. Sci.* **2024**, *11* (3), No. e2306580.
(17) Jin, X.−K.; Liang, J.−L.; Zhang, S.−M.; Huang, Q.−X.; Zhang, S.−K.; Liu, C.−J.; Zhang, X.−Z. Orchestrated copper-based nanoreactor for remodeling tumor microenvironment to amplify cuproptosis-mediated anti-tumor immunity in colorectal cancer. *Mater. Today* **2023**, *68*, 108−124.
(18) Mehta, M. M.; Weinberg, S. E.; Chandel, N. S. Mitochondrial control of immunity: beyond ATP. *Nat. Rev. Immunol.* **2017**, *17*, 608−620.
(19) Mills, E. L.; Kelly, B.; O'Neill, L. A. J. Mitochondria are the powerhouses of immunity. *Nat. Immunol.* **2017**, *18*, 488−498.
(20) Jiang, H.; Guo, Y.; Wei, C.; Hu, P.; Shi, J. Nanocatalytic innate immunity activation by mitochondrial DNA oxidative damage for tumor-specific therapy. *Adv. Mater.* **2021**, *33* (20), No. 2008065.
(21) Lu, Y.; Fan, X.; Pan, Q.; He, B.; Pu, Y. A mitochondria-targeted anticancer copper dithiocarbamate amplifies immunogenic cuproptosis and macrophage polarization. *J. Med. Chem. B* **2024**, *12*, 2006−2014.
(22) Guo, B.; Yang, F.; Zhang, L.; Zhao, Q.; Wang, W.; Yin, L.; Chen, D.; Wang, M.; Han, S.; Xiao, H.; Xing, N. Cuproptosis induced by ROS responsive nanoparticles with elesclomol and copper combined with αPD-L1 for enhanced cancer immunotherapy. *Adv. Mater.* **2023**, *35* (22), No. 2212267.
(23) Wu, H.; Zhang, Z.; Cao, Y.; Hu, Y.; Li, Y.; Zhang, L.; Cao, X.; Wen, H.; Zhang, Y.; Lv, H.; Jin, X. A self-amplifying ROS-responsive nanoplatform for simultaneous cuproptosis and cancer immunotherapy. *Adv. Sci.* **2024**, *11*, No. 2401047.
(24) Jiang, A.; Luo, P.; Chen, M.; Fang, Y.; Liu, B.; Wu, Z.; Qu, L.; Wang, A.; Wang, L.; Cai, C. A new thinking: deciphering the aberrance and clinical implication of copper-death signatures in clear cell renal cell carcinoma. *Cell. Biosci.* **2022**, *12*, 209.
(25) Yu, X.; Li, B.; Yan, J.; Li, W.; Tian, H.; Wang, G.; Zhou, S.; Dai, Y. Cuproptotic nanoinducer-driven proteotoxic stress potentiates cancer immunotherapy by activating the mtDNA-cGAS-STING signaling. *Biomaterials* **2024**, *307*, No. 122512.
(26) Tian, H.; Duan, J.; Li, B.; Qin, S.; Nice, E. C.; Zhang, W.; Lang, T.; Zhang, H.; Huang, C. Clinical chemotherapeutic agent coordinated copper-based nanoadjuvants for efficiently sensitizing cancer chemo-immunotherapy by cuproptosis-mediated mitochondrial metabolic reprogramming. *Adv. Funct. Mater.* **2023**, *33* (51), No. 2306584.
(27) Xu, M.; Chen, H.; Zhu, G.; Zhu, X.; Gao, R.; Xu, B.; Song, X.; Han, X.; Shao, T.; Sun, Q.; Xiao, Z.; Wang, H.; Zhang, Y.; Yang, G.; Li, J. Spiky metal-organic framework nanosystem for enhanced cuproptosis-mediated cancer immunotherapy. *Nano Today* **2024**, *56*, No. 102231.
(28) Navarro, M.; Cisneros-Fajardo, E. J.; Sierralta, A.; Fernández-Mestre, M.; Silva, P.; Arrieche, D.; Marchán, E. Design of copper DNA intercalators with leishmanicidal activity. *J. Biol. Inorg. Chem.* **2003**, *8*, 401−408.
(29) Draksharapu, A.; Boersma, A. J.; Leising, M.; Meetsma, A.; Browne, W. R.; Roelfes, G. Binding of copper(II) polypyridyl complexes to DNA and consequences for DNA-based asymmetric catalysis. *Dalton Trans.* **2015**, *44*, 3647−3655.
(30) Nikolić, S.; Rangasamy, L.; Gligorijević, N.; Aranđelović, S.; Radulović, S.; Gasser, G.; Grgurić-Šipka, S. Synthesis, characterization and biological evaluation of novel Ru(II)−arene complexes containing intercalating ligands. *J. Inorg. Biochem.* **2016**, *160*, 156−165.
(31) Villarreal, W.; Colina-Vegas, L.; Visbal, G.; Corona, O.; Corrêa, R. S.; Ellena, J.; Cominetti, M. R.; Batista, A. A.; Navarro, M. Copper(I)−phosphine polypyridyl complexes: synthesis, characterization, DNA/HSA binding study, and antiproliferative activity. *Inorg. Chem.* **2017**, *56*, 3781−3793.
(32) Banerjee, S.; Dixit, A.; Maheswaramma, K. S.; Maity, B.; Mukherjee, S.; Kumar, A.; Karande, A. A.; Chakravarty, A. R. Photocytotoxic ternary copper(II) complexes of histamine Schiff base and pyridyl ligands. *J. Chem. Sci.* **2016**, *128*, 165−175.
(33) Chang, J.; Yin, W.; Zhi, H.; Chen, S.; Sun, J.; Zhao, Y.; Huang, L.; Xue, L.; Zhang, X.; Zhang, T.; Dong, H.; Li, Y. Copper deposition in polydopamine nanostructure to promote cuproptosis by catalytically inhibiting copper exporters of tumor cells for cancer immunotherapy. *Small* **2024**, *20*, No. 2308565.
(34) Jia, W.; Tian, H.; Jiang, J.; Zhou, L.; Li, L.; Luo, M.; Ding, N.; Nice, E. C.; Huang, C.; Zhang, H. Brain-targeted HFn-Cu-REGO

https://doi.org/10.1021/jacsau.4c00712
JACS Au 2024, 4, 3988−3999

nanoplatform for site-specific delivery and manipulation of autophagy and cuproptosis in glioblastoma. *Small* **2023**, *19* (2), No. 2205354.
(35) Huang, Y.; Liu, X.; Zhu, J.; Chen, Z.; Yu, L.; Huang, X.; Dong, C.; Li, J.; Zhou, H.; Yang, Y.; Tan, W. Enzyme core spherical nucleic acid that enables enhanced cuproptosis and antitumor immune response through alleviating tumor hypoxia. *J. Am. Chem. Soc.* **2024**, *146* (20), 13805−13816.
(36) Sánchez-Morán, I.; Rodríguez, C.; Lapresa, R.; Agulla, J.; Sobrino, T.; Castillo, J.; Bolaños, J. P.; Almeida, A. Nuclear WRAP53 promotes neuronal survival and functional recovery after stroke. *Sci. Adv.* **2020**, *6* (41), No. eabc5702.
(37) Humphries, F.; Shmuel-Galia, L.; Ketelut-Carneiro, N.; Li, S.; Wang, B.; Nemmara, V. V.; Wilson, R.; Jiang, Z.; Khalighinejad, F.; Muneeruddin, K.; Shaffer, S. A.; Dutta, R.; Ionete, C.; Pesiridis, S.; Yang, S.; Thompson, P. R.; Fitzgerald, K. A. Succination inactivates gasdermin D and blocks pyroptosis. *Science* **2020**, *369* (6511), 1633−1637.
(38) Xu, Y.; Liu, S.−Y.; Zeng, L.; Ma, H.; Zhang, Y.; Yang, H.; Liu, Y.; Fang, S.; Zhao, J.; Xu, J.; Xu, Y.; Ashby, C. R.; He, Y.; Dai, Z.; Pan, Y. An enzyme-engineered nonporous copper(I) coordination polymer nanoplatform for cuproptosis-based synergistic cancer therapy. *Adv. Mater.* **2022**, *34* (43), No. 2204733.
(39) Guo, Y.; Tsai, H.−i.; Zhang, L.; Zhu, H. Mitochondrial DNA on Tumor-Associated Macrophages Polarization and Immunity. *Cancers* **2022**, *14*, 1452.
(40) McArthur, K.; Whitehead, L. W.; Heddleston, J. M.; Li, L.; Padman, B. S.; Oorschot, V.; Geoghegan, N. D.; Chappaz, S.; Davidson, S.; San Chin, H.; Lane, R. M.; Dramicanin, M.; Saunders, T. L.; Sugiana, C.; Lessene, R.; Osellame, L. D.; Chew, T.−L.; Dewson, G.; Lazarou, M.; Ramm, G.; Lessene, G.; Ryan, M. T.; Rogers, K. L.; van Delft, M. F.; Kile, B. T. BAK/BAX macropores facilitate mitochondrial herniation and mtDNA efflux during apoptosis. *Science* **2018**, *359*, No. eaao6047.
(41) Yu, C.−H.; Davidson, S.; Harapas, C. R.; Hilton, J. B.; Mlodzianoski, M. J.; Laohamonthonkul, P.; Louis, C.; Low, R. R. J.; Moecking, J.; De Nardo, D.; Balka, K. R.; Calleja, D. J.; Moghaddas, F.; Ni, E.; McLean, C. A.; Samson, A. L.; Tyebji, S.; Tonkin, C. J.; Bye, C. R.; Turner, B. J.; Pepin, G.; Gantier, M. P.; Rogers, K. L.; McArthur, K.; Crouch, P. J.; Masters, S. L. TDP-43 triggers mitochondrial DNA release via mPTP to activate cGAS/STING in ALS. *Cell* **2020**, *183* (3), 636−649.
(42) Wang, K.; Li, Y.; Wang, X.; Zhang, Z.; Cao, L.; Fan, X.; Wan, B.; Liu, F.; Zhang, X.; He, Z.; Zhou, Y.; Wang, D.; Sun, J.; Chen, X. Gas therapy potentiates aggregation-induced emission luminogen-based photoimmunotherapy of poorly immunogenic tumors through cGAS-STING pathway activation. *Nat. Commun.* **2023**, *14*, 2950.
(43) Huang, Y.; Qin, G.; Cui, T.; Zhao, C.; Ren, J.; Qu, X. A bimetallic nanoplatform for STING activation and CRISPR/Cas mediated depletion of the methionine transporter in cancer cells restores anti-tumor immune responses. *Nat. Commun.* **2023**, *14*, 4647.
(44) Cai, L.; Wang, Y.; Chen, Y.; Chen, H.; Yang, T.; Zhang, S.; Guo, Z.; Wang, X. Manganese(II) complexes stimulate antitumor immunity via aggravating DNA damage and activating the cGAS-STING pathway. *Chem. Sci.* **2023**, *14*, 4375−4389.
(45) Zheng, Y.; Chen, X.−X.; Zhang, D.−Y.; Wang, W.−J.; Peng, K.; Li, Z.−Y.; Mao, Z.−W.; Tan, C.−P. Activation of the cGAS-STING pathway by a mitochondrial DNA-targeted emissive rhodium(III) metallointercalator. *Chem. Sci.* **2023**, *14*, 6890−6903.
(46) Dvorkin, S.; Cambier, S.; Volkman, H. E.; Stetson, D. B. New frontiers in the cGAS-STING intracellular DNA-sensing pathway. *Immunity* **2024**, *57* (4), 718−730.

https://doi.org/10.1021/jacsau.4c00712
JACS Au 2024, 4, 3988−3999